Spring 2023

Bite Force and Stress Content of Varying Tooth Morphology and Jaw Alignment

Emily Newenhisen
een17@uakron.edu

Bite Force and Stress Content of Varying Tooth Morphology and Jaw Alignment

Emily Newenhisen

Department of Biology

The University of Akron

Williams Honors College Research Project

This study was completed by Emily Newenhisen under the guidance of Dr. Astley and graduate student Hope Zimmerman.

Abstract

Biting is one of the primary physical actions against a food substrate involved in the process of mastication and consumption. Different shapes of solidified tissue (e.g., teeth, mandibles) are developed based on dietary preferences of the organism to improve mechanical function. Models of various geometric shapes were used to loosely replicate several common biological tooth structures. As there is little research conducted on tooth penetration force in relation to tooth shape, collection of such data was the main focus of the research. Molariform teeth found in herbivores were represented by the ball model, carnivorous needle-like teeth by cone model, cutting teeth by the single blade, and thick serrated denticulation of canines by the jagged model. The question of average tooth penetration force in relation to each subclade was addressed using both a bite force rig to obtain quantitative data, as well as incorporating photoelasticity to provide supporting qualitative evidence of induced stress. Four test subjects were chosen (one model representing each tooth structure) with five trials for each subject to confirm accuracy. Orientation was then altered by testing retrognathism (overbite) and prognathism (underbite) malocclusions using a top jaw ± 10% along the x and y axis from the standard 100%. Results supported the hypothesis of decreased bite force required for acute and sharp teeth. However, results contradicted initial hypothesis of increased bite force for malocclusions.

Introduction

Consumption of proper sustenance is necessary for the survival and reproduction of all animals. Through evolution, different patterns of feeding have developed to maximize the ability to ingest the necessary material within the environment. Some organisms that reside in aquatic environments partake in filter feeding, where straining mechanisms using ciliated feeding organs are enacted to collect food particles from a suspended state (Ward & Shumway, 2004). Other organisms residing along the surface of the Earth most commonly partake in deposit feeding, where ciliated tentacles are used to collect nutrients embedded within sediments and stored within a specialized bulb prior to ingestion to remove unwanted material (Ward & Shumway, 2004). While both previous strategies rely on a more passive method of food intake with specialized appendages for collection and separation, this study focuses on the active initial biting mechanism of the bulk feeding method utilized by many organisms. Tooth morphology varies across animals, but for the purpose of this study, common tooth structures seen across many species were chosen. Shapes representing piercing, crushing, and cutting (single and multi-cuspid) morphologies were selected for testing. This study emulates the conditions of an animal with a morphologically homodont set of teeth continuously biting throughout a substrate, thereby providing insight pertaining to the force required by various dentition for full penetration.

Maximal bite force is dependent on a variety of physical and mechanical attributes of the teeth, substrate, and overall jaw anatomy. Jaw closing force can be very extreme, requiring large maxillary and mandibular muscles which are metabolically costly to build, stimulate, and maintain. By optimizing tooth shape to food mechanics, species can minimize the investment in jaw musculature. This study focuses on the force exerted by the tooth and jawbone itself rather than the muscles utilized in aiding mastication, with the assumption that lower forces result in lower demands on the muscles and are thus preferrable.

This study also factors in the effects of jaw alignment both independently and coincidingly with tooth morphology. Malocclusions are improper alignments of the upper and lower dental arches, causing atypical occlusal relationships between the crown of bottom and top jaw teeth when closing the jaw. If left untreated for an extended period of time, misalignment can lead to severe oral health complications in humans. Class 2 retrognathism malocclusions, also known as ‘overbite’, are often associated with affected consumption patterns, speech ability, and chronic oral ventilation (Buschang et al., 2007); (Grippaudo et al., 2016); (Lathrop-Marshall et al., 2021). Class 3 prognathism malocclusions, commonly referred as ‘underbite’ present similar consequences as class 2 malocclusions, but are also linked to limited motion, temporomandibular joint disfunction, and potential skeletal and tissue damage (Zere et al., 2018). While developing an underbite is less common than an overbite (1% versus 66% of United States population, respectively), the severity of such consequences is more detrimental and thus, greater efforts are dedicated towards Class 3 studies (Uribe et al., 2013) (McNamaea et al., 1996). This specific study presented bite models representing both class 2 and class 3 malocclusions when both contacting and penetrating a substrate. However, instead of highlighting differences regarding chewing patterns of malocclusion inflicted jaws, this study focuses on the differences in force exerted during initial biting for consumption, a scope not previously studied. The standard bite model utilized within this study was meant to be used as a comparison between perfect alignment and an offset of 10% from the standard at each end of the spectrum, thus falling into the most common category of misalignment of 1-4 mm offset (Pullinger and Seligman, 1991).

I hypothesized that the force required for full substrate penetration would be significantly less for tooth models of sharper edges due to the surface area of serrated edges and thin shape. Therefore, narrow models with serrated borders, specifically the cone model, are expected to see a significant decrease in exerted force for full penetration. My second hypothesis regarding jaw alignment is that there is a significant increase in force required to penetrate substrates with malocclusions. My third hypothesis is that the average jaw angle required to fully penetrate a substrate is significantly affected by sharper tooth morphology but not by jaw alignment/misalignment.

This study provides a greater understanding of the initial action of biting in animals as the amount of force required to completely slice through a substrate was compared across different geometric tooth shapes representing actual tooth morphologies. This study also delves into the affects of jaw misalignment, such as retrognathism and prognathism, commonly known as overbite and underbite, respectively, on the initial required biting forces. Potential questions within comparative anatomy and biomechanics regarding bite force and the effects of jaw misalignment can be answered from collected data.

Materials and Methods

Teeth Models

Models were obtained as both JSTAT and STL files generated by the efforts of Hope Zimmerman's previous work. The models labeled 'ball', 'cone', and 'single blade' were uploaded as STL files into MeshLab and the dovetails connecting to the base of the object were excised and exported as an STL file. When undergoing the same process with the model labeled 'jagged', tooth surface distortions occurred. To preserve occlusal, medial, and lingual surfaces of teeth, the jagged model was uploaded to AutoDesk Fusion 360 where dovetails were properly removed while maintaining the model's proper angularity and complexity. Once all dovetails were removed, models were exported as STL files to CHITUBOX, where 3D resin prints were constructed using ELEGOO Saturn S resin printer using ABS-like resin. Successful prints were washed with ethanol to remove any liquid resin coating the solid model. Once bathed, models were placed in a curing station at 60 degrees Celsius for 260 minutes. Upon completion of curing, models were structurally sound enough to undergo testing. A full set (two jaws) were printed for each type of model at standard 100% conditions. To emulate retrognathism offset biting, a single ball plate jaw was printed at conditions of x: 110%, y: 110%, z: 100% to alter solely the tooth/jaw width and, while still maintaining complexity and not altering tooth height (z-axis). Similar steps were conducted for prognathism offset biting; however, conditions were altered to x: 90%, y: 90%, z: 100% for underbite. Exact methods for preparation and printing of underbite and overbite models were conducted for all geometric tooth models.

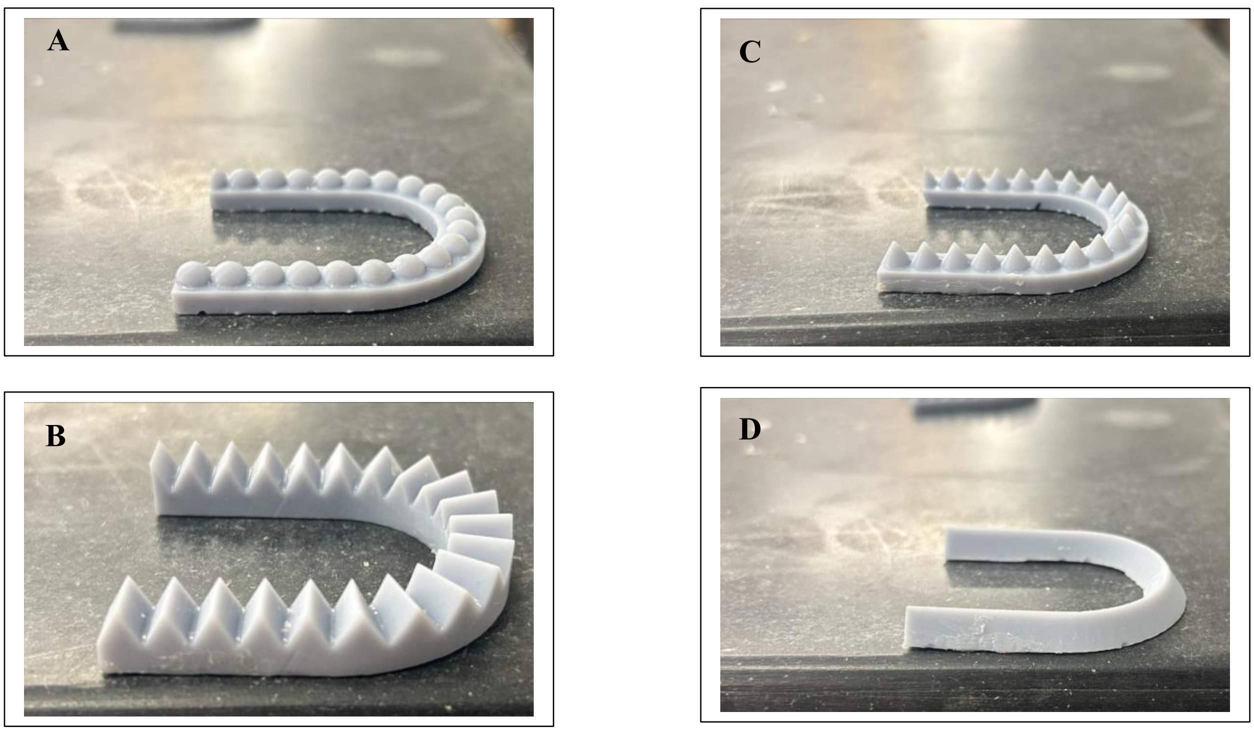

Figure 1. Tooth models used for bite force testing. Geometric shapes of ball (A), jagged (B), cone (C), and single blade (D) scaled at 100% for jaw width, jaw length, and tooth height- deemed as ‘standard.’ Overbite and underbite jaws (not depicted) were altered along the jaw width and jaw length axis.

Biting Apparatus Build

The biting rig was constructed by first cutting two 1 x 1.5 x 9 wooden boards for the platform supporting the bottom jaw. The previously cut wooden planks were fused together using epoxy, held in position using plastic clamps, and granted 15 minutes to properly cure.

Epoxy was added within cracks and openings between the wooden planks to ensure connectivity and stability of the boards. Another set of 1 x 1.5 x 7.5 wooden planks were cut and fused together for the platform housing the top jaw using the same methods of epoxy as performed for the bottom jaw platform. Once all wooden platforms were secured to one another, an outline of a standard set of jaws was traced onto the surface area 5 mm from the front edge of the planks to serve as a standard plating position. A slight indentation along all surfaces of the 7.5” platform was created using a band saw for future mass calibrations of the plank. Two light T-hinges were attached horizontally to the base of the 7.5” wooden plank, offset slightly so the edge of the plank rested on the pin on the hinge. The remaining unattached portion of the hinges were then screwed into the bottom platform at exactly 7.5”; therefore, fixating both the top and bottom wooden platforms in an aligned position to one another. The remaining 2.5” length of the lower wooden platform was used as a surface area for the grip clamp to stabilize the apparatus to the table when testing. A digital level was adhered to the top plank to determine the apparatus’ angle when in the open position. A 3.2 liter bucket attached via Kevlar rope was hung from the top platform for water collection. Both the mass of the upper wooden plank and empty hanging plastic bucket were calculated and then multiplied by gravitational constant, 9.81 m/s2, to determine the load bearing force contributed by each object onto the hinge. Values for both the mass and the calculated force for the wooden plank and plastic bucket were 294g (2,884 N) and 121g (1,187 N), respectively. Visual representation of the biting apparatus is located below in **Figure 2.**

Figure 2. Bite simulator apparatus. Photograph of apparatus used for testing bite force of jaws at both standard position and offset alignments.

Gelatin Molds

Testing substrates for biting trials were created using Knox gelatin under conditions as described in Jussila (2004). Measurements for each gelatin batch were created under conditions for 1000 mL. Exactly 100 g of Knox gelatin powder was weighed and collected in a ceramic dish for future use. About 500 mL of room temperature water was obtained in a 1000 mL flask and stirred violently, generating a whirlpool within the flask. While stirring, 100 g of gelatin was incorporated in the water. Stirring and powder incorporation were enacted simultaneously to improve saturation of the powdered gelatin. Stirring of the mixture continued until the liquid's color shifted from a bright yellow solution to a pale yellow color and all clumps of gelatin powder were broken up or dissolved. The color change of the mixture was accompanied by resistance of the material within the beaker. Once the mixture thickened and became more difficult to whisk, the material was set aside for approximately three (3) minutes to settle and congeal. While gelatin was hardening, 1 L of water was added to an electric kettle to boil. Once heated, 430 mL of boiling water was collected in a 1000 mL beaker. The remaining 70 mL of room temperature of water was added to the beaker to reach exactly 500 mL. Incorporation of both boiled and room temperature water was done to obtain 500 mL of water at exactly 50 ° F, the ideal temperature for developing gelatin with tensile strength and elasticity for accurate testing purposes. Therefore, slight modifications of each water temperature were made for each batch to obtain 50 ° F each time. Once the water reached the optimal 50 ° F, the beaker was placed on a hot plate to maintain proper temperatures. After the gelatin was granted enough time to solidify, it was transferred into the heated water and combined until gelatin fully melted into a bright yellow liquid solution. White foam and bubbles were removed from the top of the solution to ensure transparency of molds. Solution was poured into petri dishes, filling up the plastic container almost entirely, just enough to avoid overflow. Roughly fifteen petri dish molds were created with 1000 mL gelatin solution. Gelatin cooking methods were repeated seven times, resulting in 105 usable biting substrates for testing.

Data Collection and Statistics

Standard ball shaped plates were hot glued onto both top and bottom platforms at outlined positions 5 mm from the front edge of the wooden planks. The top jaw platform was lowered each time before testing to confirm jaw alignment. Once jaws were secured, a gelatin mold was carefully removed from the petri dish and placed on top of the bottom jaw plate. The top jaw platform was set at an angle of approximately 39 ° each trial to create a universal starting position. A standard 500 mL of water was added to the hanging plastic container for each trial to overcome the upward force of the hinge connecting the upper and lower platforms, thus lowering the upper platform to contact the substrate placed on top of the lower jaw and zeroing out the upward force. Additional water was added in increments of 500 mL, measuring as 4.95 N, each time until substrate was penetrated, and jaw plates contacted one another. The amount of additional water required for apparent gelatin puncturing was recorded in mL, converted into grams through the 1:1 ratio, changed into kilograms, and multiplied by gravitational constant 9.81 m/s^2 to determine the exerted force in Newtons. Jaw angles for initial penetration of substrates for each model and jaw alignment were also recorded. Photo-elastic measurements were collected using a polarized camera lens while simultaneously testing bite force to confirm stress induced by tooth penetration onto the substrate, supplying supportive qualitative data. Photos (found in Results) were analyzed through VirtualDub and chosen based on moments during testing when stress induced upon the substrate was most apparent.

Five trials (n=5) were conducted for each tooth shape under conditions of standard alignment, underbite, and overbite. Data collection was repeated under exact conditions for all four tooth shapes (ball, cone, single blade, and jagged plate). Therefore, a total of 60 trials across all testing variables were conducted. Collected data was recorded into statistical software JMP to generate statistical analysis. A two way ANOVA test was performed to compare the force required to puncture substrate and change in angles upon additional increments of water across varying tooth morphology and jaw alignment. Statistical analysis was performed to determine any significant differences between each form of jaw sets, positioned both at standard direct bite and offset overbite/underbite.

Results

Biting Force

The biting force of the jaws throughout testing substrate penetration saw a significant difference (**Figure 3.**; p-value = <0.001) across tooth morphology but did not across jaw orientation (**Figure 4.**; p-value = 0.5864). The comparison of bite force relative to both jaw alignment and tooth morphology saw no significant difference (**Figure 5.**; p-value = 0.9939). A two way ANOVA test was run and determined that there was no significant difference found when focusing on jaw alignment but highlighted a significant difference between tooth morphology when analyzing force data. Both jagged tooth model and cone model were significantly different from all treatment groups with means of 22.7 ± 0.86 Newtons and 12.01 ± 1.23 Newtons, respectively. Ball and single blade model, when compared to one another, did not significantly differ in values as the means of force exerted by the models during testing were 18.05 ± 0.98 Newtons and 18.73 ± 0.96 Newtons, respectively.

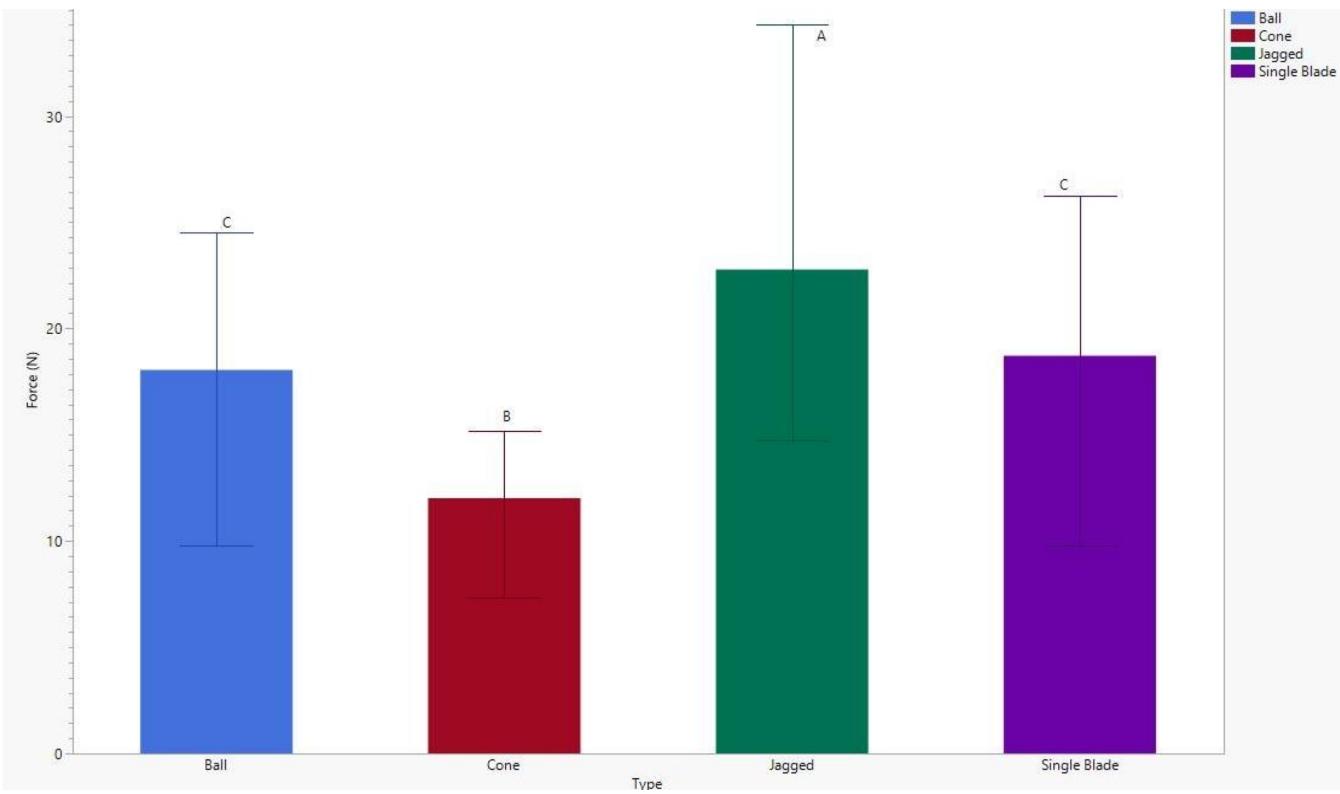

Figure 3. Bite force versus tooth structure. Measurements of average bite force recorded in Newtons across ball, cone, jagged, and single blade tooth models. Statistical analysis and plots indicate significant difference across some groups $p < 0.05$. Error bars are within one standard error of the mean value for each treatment. Symbols A, B, and C represent significant differences in bite force across testing between subjects.

The minimum angle jaw angle required for substrate penetration across jaw alignments did not differ. A two way ANOVA test was run and determined there was no significant difference found between the jaw angle of the orientations of the jaws. The mean angle value of jaws with a 110% overbite was 3.54 ± 0.1 degrees. The mean angle value of jaws with a 90% underbite was calculated as 3.67 ± 0.1 degrees. The mean angle value of jaws positioned at standard orientation and perfect alignment was determined to be 3.57 ± 0.1 degrees (**Figure 4.**).

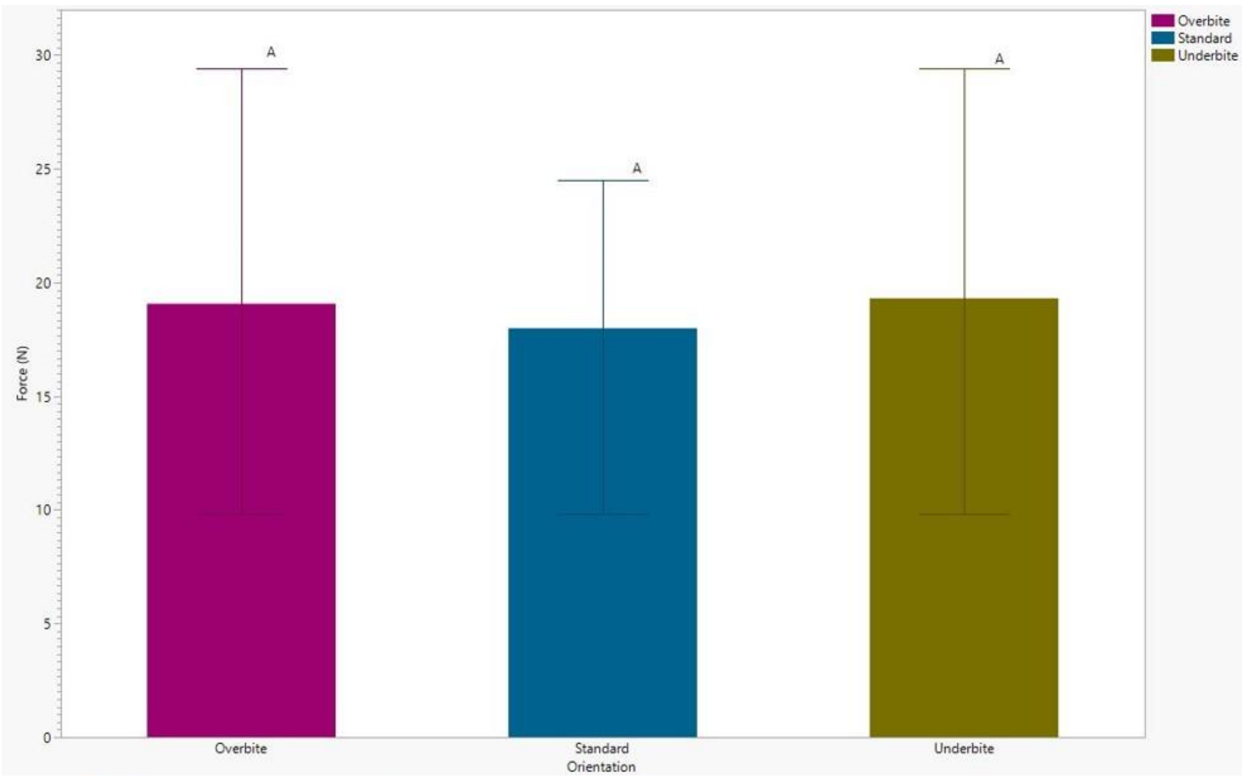

Figure 4. Bite force versus jaw alignment. Measurements of average bite force recorded in Newtons across testing models positioned at overbite (10% increase from standard), standard, and underbite (10% decrease from standard) orientations. Statistical analysis and plots indicate no significant difference across some groups $p > 0.05$. Error bars are within one standard error of the mean value for each treatment. Symbols A represents the lack of significant difference across groups.

The biting force when comparing both jaw orientation (overbite, standard, underbite) and tooth morphology (ball, cone, jagged, single blade) together saw no significant difference (**Figure 5.**; p- value = 0.9939). However, significant differences across treatment groups were present. The jagged tooth morphology, at all alignments (overbite, underbite, and standard), was significantly different from the cone structured jaw at all alignments. Jagged tooth styles presented mean force values of 22.49 ± 1.50, 23.78 ± 1.45, and 21.97 ± 1.52 Newtons at overbite, underbite, and standard positions, respectively. Cone jaw styles presented mean force values of 12.59 ± 2.09, 11.35 ± 2.15, and 12.07± 2.15 Newtons at overbite, underbite, and standard positions, respectively. Both ball and single blade models can be related to both jagged and cone models at all positions of alignment. Values regarding mean bite force values (N), as well as standard deviations for all models can be found in **Table 1.**

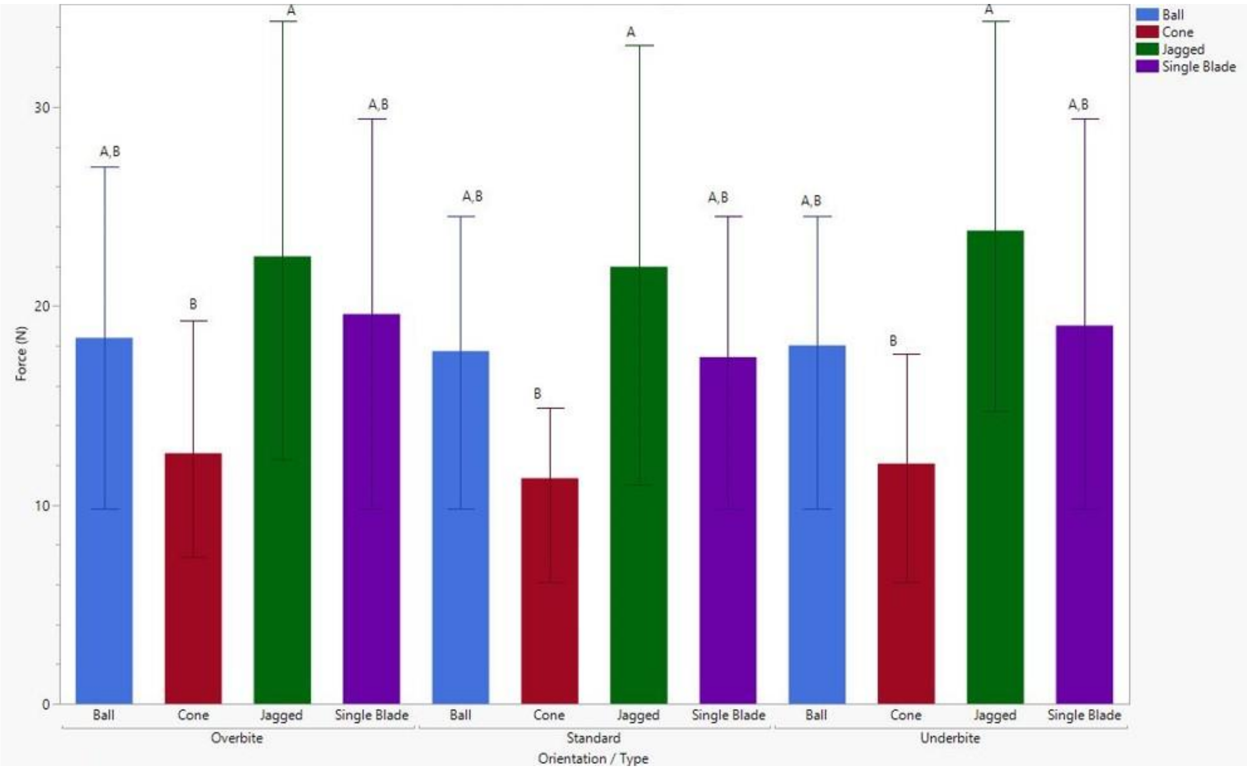

Figure 5. Bite force versus tooth structure in relation to jaw orientation. Measurements of average bite force recorded in Newtons across ball, cone, jagged, and single blade tooth models when overbite and underbite was factored into account. Statistical analysis and plots indicate significant difference across some groups $p < 0.05$. Error bars are within one standard error of the mean value for each treatment. Symbols A, B, and C represent significant differences in jaw angle across testing between subjects.

Tooth Structure	Orientation	Mean (N)	Std Dev
Jagged	Overbite	22.490488	1.4990609
Jagged	Standard	21.971750	1.5176835
Jagged	Underbite	23.778182	1.4470544
Ball	Overbite	18.386818	1.6709145
Ball	Standard	17.721290	1.7239726
Ball	Underbite	18.010500	1.6968217
Cone	Overbite	12.590000	2.0946022
Cone	Standard	11.345500	2.1463285
Cone	Underbite	12.072000	2.1463285
Single Blade	Overbite	19.592429	1.6224719
Single Blade	Standard	17.431387	1.7239726
Single Blade	Underbite	19.011618	1.6461589

Table 1. Mean and standard deviations for bite force versus tooth shape in relation to orientation.

Jaw Angle

The angle of the jaw throughout substrate penetration saw a significant difference (**Figure 6**.; p-value = <0.001) across tooth morphology but did not across jaw alignment (**Figure 7.**; p-value = 0.8859). The interaction between orientation of the jaw and type of tooth structure also saw no significant difference (**Figure 8.**; p-value = 0.4660). A two way ANOVA test was run and determined that there was no significant difference found when focusing on jaw alignment but highlighted a significant difference between tooth morphology. The jagged tooth model was significantly different across all treatment groups (cone, ball, single blade, jagged) with mean angle value of 4.39 ± 0.1 degrees. The cone tooth model, with a mean angle value of 3.42 ± 0.13 degrees, was also significantly different from all tooth models. The single blade model was significantly different from two other models in testing, both jagged and cone, but was not significantly different from the ball model. The single blade tooth model presented a mean angle value of 2.92 ± 0.1 degrees. The ball tooth model saw a significant difference when compared to the jagged and cone models but did not significantly differ in values when compared to the single blade model. The mean angle of the ball tooth model single bite trial was 3.22 ± 0.1 degrees.

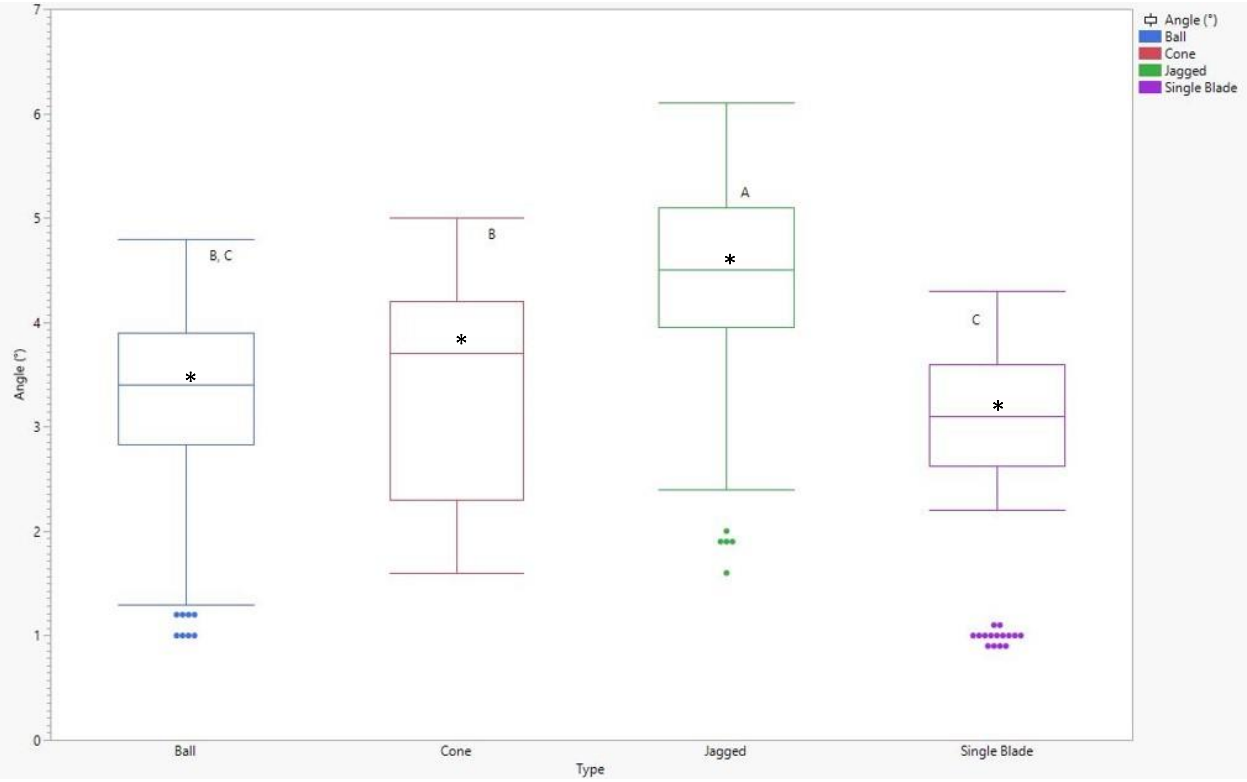

Figure 6. Jaw angle versus tooth structure. Measurements of average minimum jaw angle for substrate penetration recorded in degrees across ball, cone, jagged, and single blade tooth models. Statistical analysis and plots indicate significant difference across some groups $p < 0.05$. Error bars are within one standard error of the mean value for each treatment. Box and whisker plot illustrate the median as the solid line and the * sign as the mean. Scattered points are outliers. Symbols A, B, and C represent significant differences in minimum jaw angle for penetration across testing between subjects.

The jaw angle at overbite, direct and underbite alignments did not differ across treatment groups (**Figure 7**.) A two-way ANOVA test was run and determined there was no significant difference found between the jaw angle of the alignment of the jaws. The mean angle value of jaws with a 110% overbite was 19.07 ± 0.87 Newtons. The mean angle value of jaws with a 90% underbite was calculated as 19.31 ± 0.88 Newtons. The mean angle value of jaws positioned at standard orientation and perfect alignment was determined to be 18.00 ± 0.90 Newtons.

Figure 7. Jaw angle versus jaw alignment. Measurements of average minimum jaw angle for substrate penetration recorded in degrees across ball, cone, jagged, and single blade tooth models. Statistical analysis and plots indicate significant difference across some groups $p < 0.05$. Error bars are within one standard error of the mean value for each treatment. Box and whisker plot illustrate the median as the solid line and the * sign as the mean. Scattered points are outliers. Symbols A, B, and C represent significant differences in minimum jaw angle for penetration across testing between subjects.

The comparison of jaw pitch relative to both jaw alignment and tooth morphology saw no overall significant difference, as the p-value was greater than 0.05 (**Figure 8.**; p-value = 0.4660). However, slight significant differences across treatment groups in relation to mandibular and maxilla protrusion were determined using a two-way ANOVA test. The ball, cone, and single blade treatment groups at each position of 110% overbite, standard 100%, and 90% underbite saw no significant differences when compared to one another. Specific cone models of standard and underbite are comparable to data collected by the standard jagged model; however, only the standard cone model can be comparable across all jagged orientations. The jagged models are significantly different from both ball and single blade models at all positions, as well as the cone model at overbite and underbite placements. Means and standard deviations for each of the models with respect to jaw alignment are listed in **Table 2.**

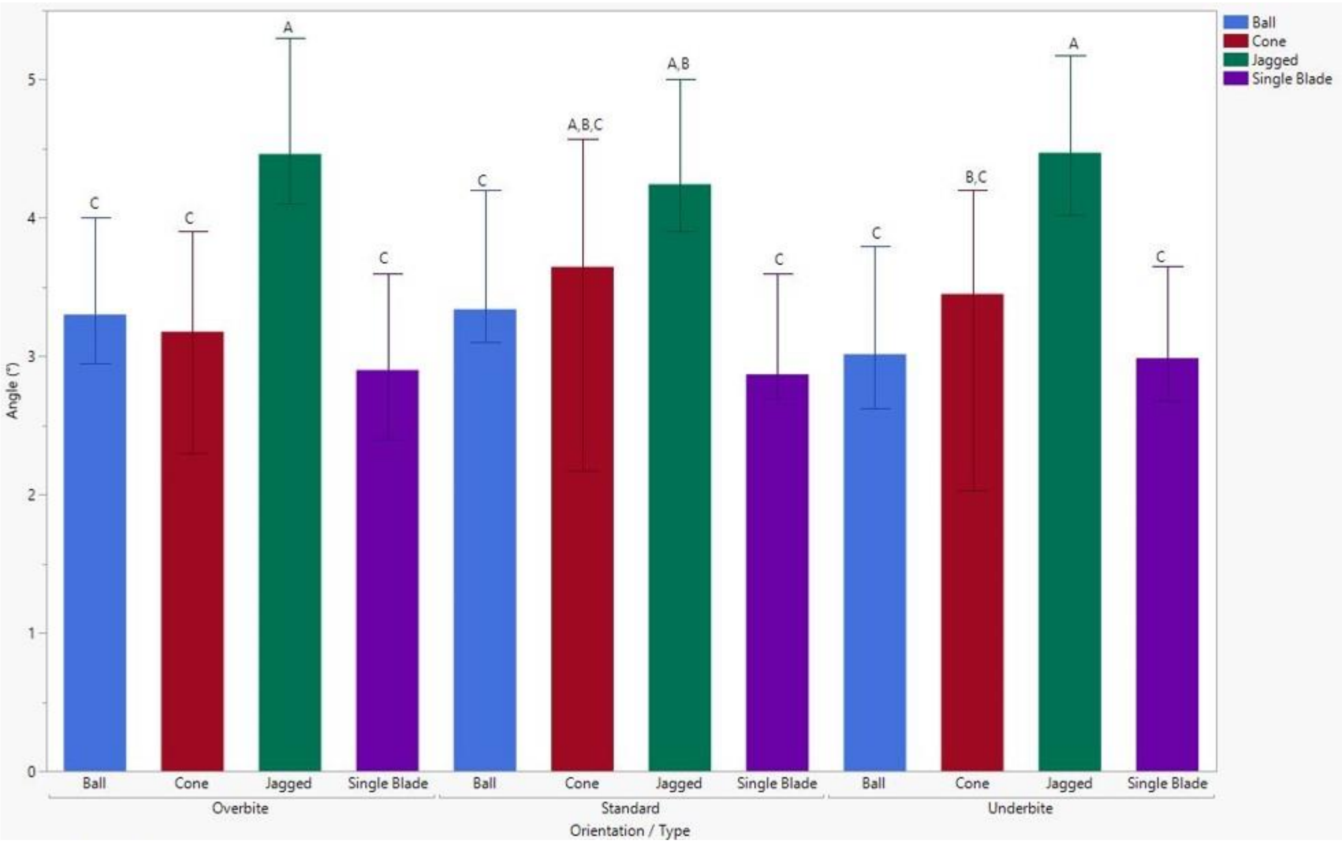

Figure 8. Jaw angle versus tooth structure in relation to jaw orientation. Measurements of average minimum jaw angle for substrate penetration recorded in degrees across ball, cone, jagged, and single blade tooth models when overbite and underbite are factored in account together. Error bars are within one standard error of the mean value for each treatment. Symbols A, B, and C represent significant differences in minimum jaw angle for penetration across testing between subjects.

Tooth Shape	Orientation	Mean (°)	Std Dev
Jagged	Overbite	4.460976	0.15919429
Jagged	Standard	4.242500	0.16117194
Jagged	Underbite	4.470455	0.15367141
Ball	Overbite	3.300000	0.17744446
Ball	Standard	3.338710	0.18307902
Ball	Underbite	3.015625	0.18019570
Cone	Overbite	3.176190	0.22243841
Cone	Standard	3.645000	0.22793154
Cone	Underbite	3.450000	0.22793154
Single Blade	Overbite	2.900000	0.17230005
Single Blade	Standard	2.867742	0.18307902
Single Blade	Underbite	2.985294	0.17481551

Table 2. Mean and standard deviations for jaw angle versus tooth shape in relation to orientation.

Photo-elastic measurements

Stress exerted upon substrate during testing was collected for each of the treatment groups using the whole-field technique of photoelasticity. Photoelasticity visualizes the mechanical deformations of material when undergoing pressure, illuminating the distribution of stress experienced across the substrate. Visualization of a substance's stress content is possibly due to the temporary double refraction of light rays, called birefringence, generated from light rays crossing one another in a perpendicular fashion (Ramesh 2021). Results of clashing light rays are depicted as an array of colors oriented at specific locations that underwent stress. Photo-elastic measures were collected as a qualitative value to confirm stress was induced upon the substrate when contacted by jaw structures. Photographs of photoelasticity were collected during the halfway point of each trial, when a considerable amount of force was displaced along points of contact within the gelatin.

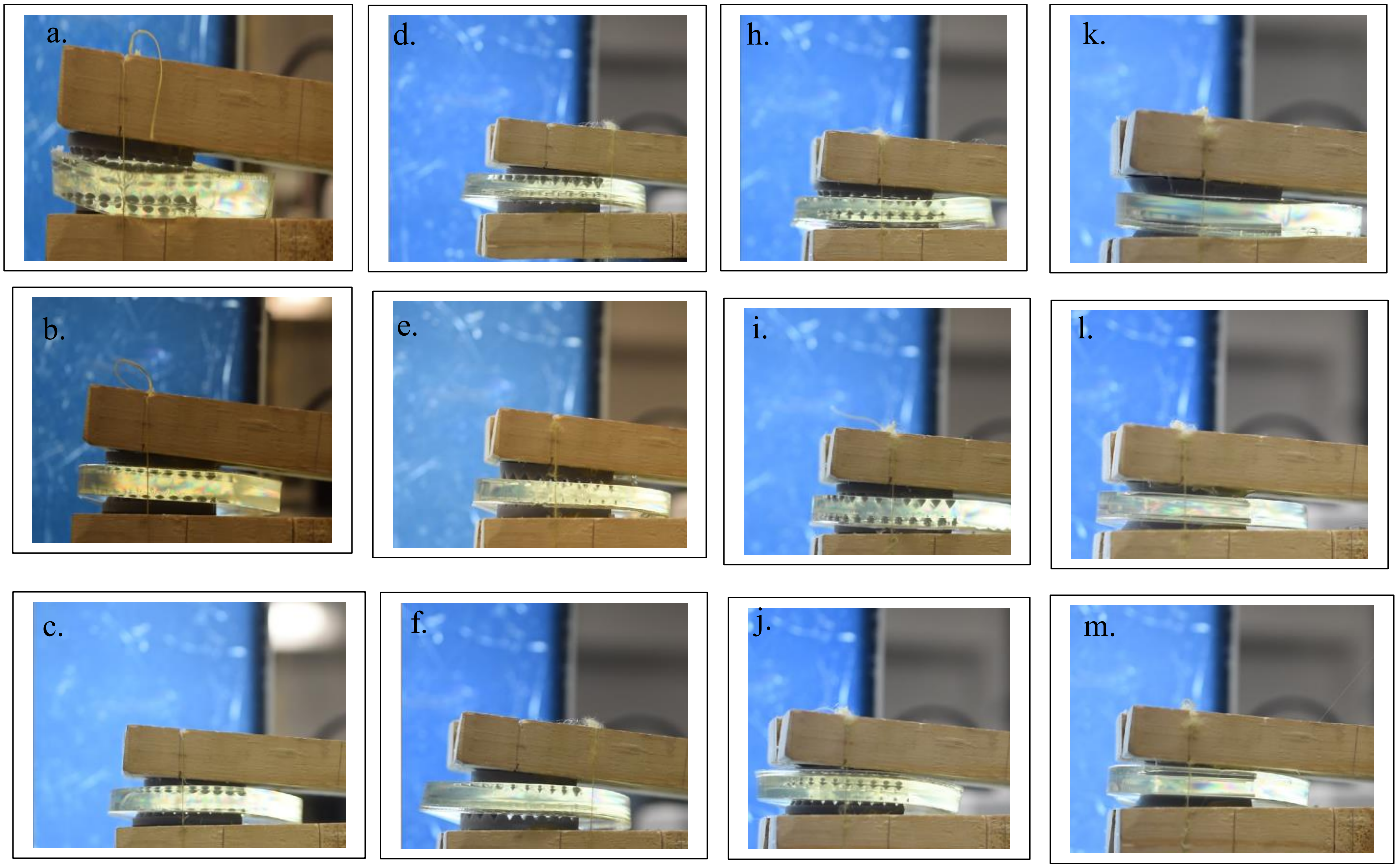

Figure 9. Examples of photoelasticity during trials for each tooth model at each orientation. Photographs a-c depict the overbite, standard, and underbite orientations of the ball jaw set, respectively. Pattern was repeated for jagged (e-f), cone (h-j), and single blade (k-m).

Discussion

Bite force required for various tooth morphology saw significant difference across tooth models. Data indicated that the cone model experienced a decreased amount of force for complete substrate penetration that was significantly different across all other test models (**Figure 3.**; p=0.0001). The jagged model saw significantly different values much like the cone model but on the opposite end of the spectrum as it required the most force for penetration. Initially, one may assume that the jagged model would have exhibited similar results as the cone model due to its similar serrated edges. However, both the jagged edges and tooth as a whole possessed a greater surface area than the cone model. The increased support of the jagged teeth, as well as the increased surface area, may have allowed for the exerted force by the jaws to be more uniformly distributed across the substrate. As the cone model was able to apply a force more acutely along the substrate, complete piercing of the substrate may have been able to be accomplished at a reduced force when compared to other thicker models. The maximum required force to occlusal contact of the cone model was approximately half of the average maximum required force for the jagged model. Both the ball and single blade model possessed relatively similar thick dull shapes and thus presented similar average maximum bite force for substrate penetration. It has been determined that blade sharpness and penetrative force are inversely proportional; therefore, as the sharpness of the blade increases, the required force decreases (Zhou and McMurray, 2009). Through analysis of all collected data for tooth morphology alone and external experimental support regarding force and blade sharpness, the hypothesis that thin sharp tooth models with a small surface area require less force for total penetration than thicker and duller tooth models.

However, the hypothesis of bite force increasing significantly for both overbite and underbite malocclusions was not supported by the results. While results visually reported a slight decrease of average maximum force for jaws at standard orientation and slightly greater values for jaws with an underbite, there was not enough diversity across values to be deemed substantial (**Figure 4.**; p=0.4700). This directly opposes the study of Bakke (2006) which indicated that increased force would occur as decreased occlusal surfaces were expected to align and touch properly. The direct opposition of the two studies may be due to this study's chosen percent increase and decrease in malocclusion. Only a 10% variation from standard 100% alignment was chosen for overbite and underbite models as such values fell within the common 1-4 mm offset range (Pullinger and Seligman, 1991). It may be expected that an increased percent in malocclusions, such as 25-30%, falling into the severe range, would potentially alter results to more closely align with the numerous studies of bite force of malocclusion inflicted jaws.

The final hypothesis of jaw angle being significantly different for tooth morphology but not jaw misalignment was supported by the results. Jaw pitch was measured at the angle generated when a standard force of 4.59 N was applied incrementally. The jagged model angle was significantly different from all other testing models with an average angle required for complete puncturing of 4.394 degrees (**Figure 6.**; p=0.0001). The ball model shared similar results with both the cone and single blade models; however, the cone and single blade average angles were significant from one another. Studies regarding freshwater fish, Cichlid, identified significant increase of jaw angle in the fish specific carnivorous subclade when compared to herbivorous and omnivorous subclades (Sage and Selandar, 1975). This correlated with the collected data as the jagged model, similar in shape to carnivorous cichlid teeth with fish specific diets, was significantly larger than other values. However, this study demonstrates no significant difference across collected jaw angles for overbite, standard, and underbite (**Figure 7.**). A study performed by Dibbets (1996) analyzed both the craniofacial angle and mandibular angle in relation to malocclusions. While midface and cranial face malocclusions significantly differed from one another, it was discovered that the maxilla angle did not report significantly different values when testing, therefore supporting results collected within this study.

Conclusion

The comparison of bite force and jaw angle across geometric tooth shapes representing both mammalian and aquatic tooth morphologies of molariform, incisor, canine, and needle-like shapes and misalignment of jaws were used to determine if a specific tooth shape or orientation is able to penetrate a substrate easier. From analysis of data, it was determined that teeth with acute and sharp surface areas were able to completely permeate the gelatin substrate at considerably less force than all other tested models. It was also discovered that there was no considerable variation between class 2 and 3 malocclusions when compared to standard alignment, However, it was addressed that a potential reasoning for such outcome was the variation may have been too small to elicit significant results. Increasing malocclusion variation larger than 20% to fall within severe range (Pullinger and Seligman, 1991) is recommended before acceptance current results. Finally, results depicted minimum jaw angle required for substrate penetration was significant across tooth morphology but not across jaw alignment. It is possible that similar results may occur across biologically accurate jaw models under exact testing schematics. General application of this study's results is sufficient but specific biological CT jaw scans should be 3D printed and tested to derive accurate bite force and jaw angle values for both standard alignment and malocclusions of a particular test subject.

Acknowledgements

I would like to express my gratitude to Dr. Astley for both his guidance on this project and use of his lab and materials for testing. I would also like to thank graduate student Hope Zimmerman for providing me with the models to 3D print for testing as well as mentoring me throughout this entire experience. Appreciation is extended to both graduate students Kaelyn Gamel and Sam Edwards as well. Additionally, I am grateful to my father, Richard Newenhisen, who accompanied and assisted me when testing my apparatus. Thank you to the Honors faculty advisor, Dr. Bagatto, as well as readers, Dr. Olson and Dr. Duff, for your support.

Literature Cited

Bakke, M. 2006. Bite force and occlusion. Seminars in Orthodontics. 12(2): 120-126.

Buschang, P., Throckmorton, G., Austin, D., Wintergerst, A. 2007. Chewing cycle kinematics of subjects with deepbite malocclusion. *American Journal of Orthodontics and Dentofacial Orthopedics*. 131(5): 627-634.

Dibbets, J. 1996. Morphological associations between the angle classes. European Journal of Orthodontics. 18(2) 111-118.

Grippaudo, C., Paolantonio, E.G., Antonini, G., Saulle, R., La Torre, G., Deli, R. 2016. Association between oral habits, mouth breathing, and malocclusion. *ACTA Otorhinolaryngol Italica*. 36(5): 386-394.

Lathrop-Marshall, H., Keyser, M., Jhingree, S., Giduz, N., Bocklage, C., Couldwell, S., Edwards, H., Glesener, T., Moss, K., Fraizer-Bowers, S., Phillips, C., Turvey, T., Blakey, G., White, R., Mielke, J., Zajac, D., Jacox, L. 2021.Orthognathic speech pathology: impacts of Class III malocclusion on speech. *European Jounral of Orthodontics*. 44(3): 340-351.

McNamara, J., Peterson, J., & Alexander, R. 1996. Three-dimensional diagnosis and management of class II malocclusion in the mixed dentition. *Seminars in Orthodontics*. 2(2): 114–137.

Pullinger, A., & Seligman, D. 1991. Overbite and overjet characteristics of refined diagnostic groups of temporomandibular disorder patients. American Journal of Orthodontics and Dentofacial Orthopedics. 100(5): 401-415.

Ramesh, K. 2021. Basics of photoelasticity and photoelasticity. Renaissance. 1(1): 1-24.

Sage, R., & Selandar, R. 1975. Tropic radiation through polymorphism in cichlid fish. Developmental Biology. 72(11): 4669-4673.

Ward, J., & Shumway, S. 2004. Separating the grain from the chaff: particle selection and suspension- and deposit- feeding bivalves. Journal of Experimental Marine Biology and Ecology. 300(1-2): 83-130.

Uribe, L., Vela, K., Kummet, K., Dawson, D., Southhard, T. 2013. Phenotypic diversity in white adults with moderate to severe Class III malocclusion. *American Journal of Orthodontics and Dentofacial Orthopedics*. 144(1): 32-42.

Zere, E., Chaudhari, P.K., Shara, J., Dhingra, K., Tiwari, N. 2018. Developing Class III malocclusions: challenges and solutions. *Clinical, Cosmetic, and Investigational Dentistry*. 10:99-116.

Zhou, D., & McMurray, G. 2010. Modeling of blade sharpness and compression cut of biomaterials. *Robotica*. 28(2): 311-319.